Bloch-sphere colorings and Bell inequalities

Adrian Kent[1,2] and Damián Pitalúa-García[1]

[1]*Centre for Quantum Information and Foundations, DAMTP, Centre for Mathematical Sciences, University of Cambridge, Wilberforce Road, Cambridge CB3 0WA, United Kingdom*

[2]*Perimeter Institute for Theoretical Physics, 31 Caroline Street North, Waterloo, Ontario, Canada N2L 2Y5*

(Received 14 September 2014; published 18 December 2014)

We consider the quantum and local hidden variable (LHV) correlations obtained by measuring a pair of qubits by projections defined by randomly chosen axes separated by an angle θ. Local hidden variables predict binary colorings of the Bloch sphere with antipodal points oppositely colored. We prove Bell inequalities separating the LHV predictions from the singlet quantum correlations for $\theta \in (0, \frac{\pi}{3})$. We raise and explore the hypothesis that, for a continuous range of $\theta > 0$, the maximum LHV anticorrelation is obtained by assigning to each qubit a coloring with one hemisphere black and the other white.

DOI: 10.1103/PhysRevA.90.062124 PACS number(s): 03.65.Ud

I. INTRODUCTION

According to quantum theory, spacelike separated experiments performed on entangled particles can produce outcomes whose correlations violate Bell inequalities [1] that would be satisfied if the experiments could be described by local hidden variable theories (LHVTs). Many experiments have tested the quantum prediction of nonlocal causality (see, e.g., [2–8]). The observed violations of Bell inequalities are consistent with quantum theory. They refute LHVTs with overwhelmingly high degrees of confidence, modulo some known loopholes that arise from the difficulty in carrying out theoretically ideal experiments, most notably the locality loophole (closed in [2–4]), the detection efficiency loophole [9] (closed in [5,6,8]), and the collapse locality loophole [10] (addressed in [7], though not fully closed).

Typically, Bell experiments test the Clauser-Horne-Shimony-Holt (CHSH) inequality [11] in an Einstein-Podolsky-Rosen (EPR) -Bohm experiment [12,13] in which two entangled particles are sent to different experimental setups at different locations. One setup is controlled by Alice, who performs one of two possible measurements $A \in \{0,1\}$, the other by Bob, who similarly performs $B \in \{0,1\}$. Alice's and Bob's outcomes a and b are assigned numerical values $a,b \in \{1,-1\}$, corresponding to spin up or spin down for spin measurements about given axes on spin-$\frac{1}{2}$ particles. The experiments must be completed at spacelike separated regions. The experiment is repeated many times, ideally under identical experimental conditions. We define the correlation $C(A,B)$ as the average value of the product of Alice's and Bob's outcomes in experiments where measurements A and B are chosen.

According to deterministic LHVTs, the outcomes a and b are determined respectively by the measurement choices A and B and by hidden variables λ shared by both particles. Thus, $a = a(A,\lambda)$ and $b = b(B,\lambda)$. An LHVT also assigns a probability distribution $\rho(\lambda)$, independent of A and B, to the hidden variables, satisfying $\rho(\lambda) \geqslant 0$ and $\int_\Lambda d\lambda\, \rho(\lambda) = 1$, where Λ is the sample space of hidden variables. Probabilistic LHVTs can be described by the same equations, extending the definitions of λ and ρ to allow for probabilistic measurement outcomes; we can thus focus on deterministic LHVTs without loss of generality. An LHVT predicts $C(A,B) = \int_\Lambda d\lambda\, \rho(\lambda) a(A,\lambda) b(B,\lambda)$. Such correlations satisfy the CHSH inequality [11] $I_2 = |C(0,0) + C(1,1) + C(1,0) - C(0,1)| \leqslant 2$.

Consider for definiteness the EPR-Bohm experiment performed on spin-$\frac{1}{2}$ particles in the singlet state $|\Psi^-\rangle = \frac{1}{\sqrt{2}}(|\uparrow\rangle|\downarrow\rangle - |\downarrow\rangle|\uparrow\rangle)$. Alice and Bob measure their particle spin projection along the directions $\vec{a}_A$ and $\vec{b}_B$, respectively. As before, Alice and Bob choose a measurement from a set of two elements, that is, $A,B \in \{0,1\}$. In general, the vectors $\vec{a}_A$ and $\vec{b}_B$ can point along any direction in three-dimensional Euclidean space and the sets of their possible values define Bloch spheres $\mathbb{S}^2$. The correlation predicted by quantum theory is $Q(\theta) = -\cos\theta$, where $\cos\theta = \vec{a}_A \cdot \vec{b}_B$. Sets of measurement axes can be found for which the quantum correlations violate the CHSH inequality $I_2^{\mathrm{QM}} > 2$ up to the Cirel'son [14] bound $I_2^{\mathrm{QM}} \leqslant 2\sqrt{2}$.

When Alice's and Bob's measurement choices belong to a set of N possible elements, the correlations predicted by LHVTs satisfy the Braunstein-Caves inequality [15]

$$I_N = \left| \sum_{k=0}^{N-1} C(k,k) + \sum_{k=0}^{N-2} C(k+1,k) - C(0,N-1) \right| \leqslant 2N-2. \quad (1)$$

The CHSH inequality is a special case of the Braunstein-Caves inequality with $N = 2$. We are interested here in exploring Bell inequalities that generalize the CHSH and Braunstein-Caves inequalities, in the following sense. Instead of restricting Alice's and Bob's measurement choices to a finite set, we allow them to choose any spin measurement axes $\vec{a}$ and $\vec{b}$. However, we constrain these axes to be separated by a fixed angle θ, so $\cos\theta = \vec{a} \cdot \vec{b}$. The maximal violation of the Braunstein-Caves inequality by quantum correlations, given by $I_N^{\mathrm{QM}} = 2N\cos(\frac{\pi}{2N})$ [16], arises for fixed sets of pairs of axis choices that satisfy this constraint with $\theta = \frac{\pi}{2N}$. We consider experiments where pairs of axes separated by θ are chosen randomly and θ is unrestricted. Our work contributes to understanding how to quantify quantum nonlocality, by studying a natural class of Bell inequalities. As well as proving different inequalities, our work raises questions and suggests techniques that we hope will be developed further.

 ©2014 American Physical Society

Another more practical motivation is to explore simple Bell tests that might allow quantum theory and LHVT to be distinguished somewhat more efficiently, particularly in the adversarial context of quantum cryptography. Here an eavesdropper and/or malicious device manufacturer may be trying to spoof the correlations of a singlet using locally held or generated information. Of course, given sufficient guarantees about the devices involved, modulo the loopholes mentioned above and with sufficiently many runs, any Bell test can expose such spoofing. However, in practical situations in which the number of possible tests is limited, users would like to ensure that such eavesdropping attacks can be detected as efficiently as possible. Standard CHSH tests simplify the eavesdropper's problem, by informing her in advance that she need only generate outcomes for a small set of possible measurements. By comparison, tests involving randomly chosen axes give the eavesdropper no such information.[1] A first step towards understanding Alice's and Bob's optimal test strategy in such contexts is to identify the full range of Bell inequalities available.

II. BLOCH-SPHERE COLORINGS AND CORRELATION FUNCTIONS

We explore LHVTs in which Alice's and Bob's spin measurement results are given by $a(\vec{a},\lambda)$ and $b(\vec{b},\lambda)$, respectively; where λ is a local hidden variable common to both particles. For fixed λ, we can describe the functions a and b by two binary (black and white) colorings of spheres, associated with a and b, respectively, where black (white) represents the outcome 1 (-1). Different sphere colorings are associated with different values of λ. To look at specific cases, we drop the λ dependence and include a label x that indicates a particular pair of coloring functions $a_x(\vec{a})$ and $b_x(\vec{b})$.

Measuring spin along $\vec{a}$ with outcome 1 (-1) is equivalent to measuring spin along $-\vec{a}$ with outcome -1 (1). The coloring functions a and b defining any LHVT are thus necessarily *antipodal* functions

$$a_x(\vec{a}) = -a_x(-\vec{a}), \quad b_x(\vec{b}) = -b_x(-\vec{b}) \tag{2}$$

for all $\vec{a},\vec{b} \in \mathbb{S}^2$.

We notice that the antipodal property arises due to the definition of a dichotomic measurement on the sphere for arbitrary deterministic LHVTs. For an arbitrary probabilistic theory, this property would read

$$P_x(\mu a,\nu b|\mu\vec{a},\nu\vec{b}) = P_x(a,b|\vec{a},\vec{b}), \tag{3}$$

where $\mu,\nu,a,b \in \{\pm 1\}$; $\vec{a},\vec{b} \in \mathbb{S}^2$; and the label x indicates a particular probabilistic theory being considered. Equation (3) holds because a measurement is defined by a pair of opposite axes $\vec{a}$ and $-\vec{a}$ and inverting their sense corresponds only to relabeling the measurement outcomes.

[1]One possibility here is for Alice and Bob to fix in advance the value of θ and a list of random pairs of axes separated by θ. Another would be to make random independent choices and then generate plots of the correlations as a function of θ. This second type of test would be generated automatically by quantum key distribution schemes that require Alice and Bob to make completely random measurements on each qubit (see, e.g., [17]).

FIG. 1. Some antipodal coloring functions a_x on the sphere, see Appendix C for definitions. Their correlations $C_x(\theta)$, computed from Eq. (4), subject to the constraint (6), are plotted in Appendix C.

We define $\mathcal{X}$ as the set of all colorings x satisfying the antipodal property (2). For example, a simple coloring of the spheres satisfying the antipodal property is coloring 1, in which, for one sphere, one hemisphere is completely black and the other one is completely white and the coloring is reversed for the other sphere (see Fig. 1).

The correlation for outcomes of measurements about randomly chosen axes separated by θ for the pair of coloring functions labeled by x is

$$C_x(\theta) = \frac{1}{8\pi^2}\int_{\mathbb{S}^2} dA\, a_x(\vec{a}) \int_0^{2\pi} d\omega\, b_x(\vec{b}), \tag{4}$$

where dA is the area element of the sphere corresponding to Alice's axis $\vec{a}$ and ω is an angle in the range $[0,2\pi]$ along the circle described by Bob's axis $\vec{b}$ with an angle θ with respect to $\vec{a}$. A general correlation is of the form $C(\theta) = \int_{\mathcal{X}} dx\, \mu(x) C_x(\theta)$, where $\mu(x)$ is a probability distribution over $\mathcal{X}$.

If all colorings $x \in \mathcal{X}$ satisfy $Q_{\rho_{\mathrm{L}}}(\theta) < C^{\mathrm{L}}(\theta) \leqslant C_x(\theta)$ or $C_x(\theta) \leqslant C^{\mathrm{U}}(\theta) < Q_{\rho_{\mathrm{U}}}(\theta)$ for quantum correlations $Q_{\rho_{\mathrm{L}}}(\theta)$ and $Q_{\rho_{\mathrm{U}}}(\theta)$ obtained with particular two-qubit states ρ_{U} and ρ_{L} and some identifiable lower and upper bounds $C^{\mathrm{L}}(\theta)$ and $C^{\mathrm{U}}(\theta)$, respectively, then a general correlation $C(\theta)$ must satisfy the same inequalities. Our aim here is to explore this possibility via intuitive arguments and numerical and analytic results. We focus on the case $\rho_{\mathrm{L}} = |\Psi^-\rangle\langle\Psi^-|$, for which $Q_{\rho_{\mathrm{L}}}(\theta) \equiv Q(\theta) = -\cos\theta$, which is the maximum quantum anticorrelation for a given angle θ (see Sec. V for details and related questions). We begin with some suggestive observations.

First, we consider coloring functions $x \in \mathcal{X}$ for which the probability that Alice and Bob obtain opposite outcomes when they choose the same measurement, averaged uniformly over all measurement choices, is

$$P(a_x = -b_x|\theta = 0) = 1 - \gamma. \tag{5}$$

In general, $0 \leqslant \gamma \leqslant 1$. We first consider small values of γ and seek Bell inequalities distinguishing quantum correlations for the singlet from classical correlations for which an anticorrelation is observed with probability $1-\gamma$ when the same measurement axis is chosen on both sides. Experimentally, we can verify quantum nonlocality using these results if we carry out nonlocality tests that include some frequency of anticorrelation tests about a randomly chosen axis (chosen independently for each test). The anticorrelation tests allow statistical bounds on γ, which imply statistical tests of nonlocality via the γ-dependent Bell inequalities.

In the limiting case $\gamma = 0$, we have

$$a_x(\vec{a}) = -b_x(\vec{a}) \tag{6}$$

for all $\vec{a} \in \mathbb{S}^2$. This case is quite interesting theoretically, in that one might hope to prove stronger results assuming perfect

anticorrelation. We describe some numerical explorations of this case below.

Second, for any pair of colorings $x \in \mathcal{X}$ and $\theta \in [0,\pi]$, we have $C_x(\pi-\theta) = -C_x(\theta)$. This can be seen as follows. For a fixed $\vec{a}$, the circle with angle $\theta = \theta'$ around the axis $\vec{a}$, defined by the angle ω in Eq. (4), contains a point $\vec{b}$ that is antipodal to a point on the circle with angle $\theta = \pi - \theta'$ around $\vec{a}$. Since the coloring is antipodal, we have that the value of the integral $\int_0^{2\pi} d\omega\, b_x(\vec{b})$ in Eq. (4) for $\theta = \theta'$ is the negative of the corresponding integral for $\theta = \pi - \theta'$. It follows that $C_x(\pi-\theta') = -C_x(\theta')$. Therefore, in the rest of this paper, we restrict consideration to correlations for the range $\theta \in [0, \frac{\pi}{2}]$, unless otherwise stated. From the previous argument we have $C_x(\frac{\pi}{2}) = -C_x(\frac{\pi}{2})$, which implies that $C_x(\frac{\pi}{2}) = 0$. We also have that $C_x(0) = 1 - 2P(a_x = -b_x|\theta = 0)$, so the LHVTs we consider give $C_x(0) = -1 + 2\gamma$. The local hidden variable (LHV) correlations given by Eqs. (4) and (5) in the case $\gamma = 0$ thus coincide with the singlet-state quantum correlations for $\theta = 0$ and $\theta = \frac{\pi}{2}$, where $Q(0) = C_x(0) = -1$ and $Q(\frac{\pi}{2}) = C_x(\frac{\pi}{2}) = 0$.

Third, consider coloring 1, defined above. We have $C_1(\theta) = -(1 - \frac{2\theta}{\pi})$ for $\theta \in [0, \frac{\pi}{2}]$. This is easily seen as follows. For any two different points on the spheres defining coloring 1, $\vec{a}$ in one sphere and $\vec{b}$ in the oppositely colored one, an arc of angle π of the great circle passing through $\vec{a}$ and $\vec{b}$ is completely black and the other arc of angle π is completely white. Thus, given that the pair of vectors $\vec{a}$ and $\vec{b}$ are chosen randomly, subject to the constraint of angle separation θ, the probability that both $\vec{a}$ and $\vec{b}$ are in oppositely colored regions is $P(a_1 = -b_1|\theta) = \frac{\pi-\theta}{\pi} = 1 - \frac{\theta}{\pi}$. Thus, the correlation for coloring 1 is $C_1(\theta) = 1 - 2P(a_1 = -b_1|\theta) = -1 + \frac{2\theta}{\pi}$. That is, $C_1(\theta)$ linearly interpolates between the values at $C_1(0) = -1$, which is common to all colorings with $\gamma = 0$, and $C_1(\frac{\pi}{2}) = 0$, which is common to all colorings, and we have $0 > C_1(\theta) > Q(\theta)$ for $\theta \in (0, \frac{\pi}{2})$.

Then, in the following section we present some lemmas and a theorem.

III. HEMISPHERICAL COLORING MAXIMALITY HYPOTHESES

In this section, we motivate two hemispherical coloring maximality hypotheses. These make precise the intuition that, for a continuous range of $\theta > 0$, the maximum LHV anticorrelation is obtained by coloring 1. We first consider the following lemmas, whose proofs are given in Appendix A.

Lemma 1. For any coloring $x \in \mathcal{X}$ satisfying Eq. (5) and any $\theta \in (0, \frac{2\pi}{3}]$, we have $-1 + \frac{2}{3}\gamma \leqslant C_x(\theta) \leqslant \frac{1}{3} + \frac{2}{3}\gamma$.

Remark 1. Unsurprisingly, since small γ implies near-perfect anticorrelation at $\theta = 0$, we see that for $\theta \in (0, \frac{2\pi}{3}]$ and γ small there are no colorings with very strong correlations. However, strong anticorrelations are possible for small θ. We are interested in bounding these.

Lemma 2. For any coloring $x \in \mathcal{X}$ satisfying Eq. (5), any integer $N > 2$, and any $\theta \in [\frac{\pi}{N}, \frac{\pi}{N-1})$, we have $C_x(\theta) \geqslant C_1(\frac{\pi}{N}) - 2\gamma$.

Remark 2. In other words, for small θ, $C_1(\theta)$ is very close to the maximal possible anticorrelation for LHVTs when $\gamma \ll \theta$.

Geometric intuitions also suggest bounds on $C_x(\theta)$ that are maximized by coloring 1 for small θ. Consider *simple colorings*, in which a set of (not necessarily connected) piecewise differentiable curves of finite total length separate black and white regions. (Points lying on these curves may have either color.) Intuition suggests that, for small θ and simple colorings with $\gamma = 0$, the quantity $1 + C_x(\theta)$, which measures the deviation from pure anticorrelation, should be bounded by a quantity roughly proportional to the length of the boundary between the black and white areas of the sphere coloring $x \in \mathcal{X}$. Since coloring 1 has the smallest such boundary (the equator), this might suggest that $C_x(\theta) \geqslant C_1(\theta)$ for small θ and for all simple colorings $x \in \mathcal{X}$ with $\gamma = 0$. Intuition also suggests that any nonsimple coloring will produce less anticorrelation than the optimal simple coloring, because regions in which black and white colors alternate with arbitrarily small separation tend to wash out anticorrelation. These intuitive arguments are clearly not rigorous as currently formulated. For example, they ignore the possibility of sequences of colorings $C_i(\theta)$ and angles $\theta_i \to 0$ such that $C_i(\theta_i) < C_1(\theta_i)$, while $\lim_{\theta\to 0}[C_i(\theta) - C_1(\theta)] > 0$ for all i (see [18] for an extended discussion). Still, they are suggestive, at least in generating hypotheses to be investigated.

These various observations motivate us to explore what we call the weak hemispherical coloring maximality hypothesis (WHCMH).

The WHCMH. There exists an angle $\theta^{\mathrm{w}}_{\max} \in (0, \frac{\pi}{2})$ such that for every coloring $x \in \mathcal{X}$ with $\gamma = 0$ and every angle $\theta \in [0, \theta^{\mathrm{w}}_{\max}]$, $C_x(\theta) \geqslant C_1(\theta)$.

The WHCMH considers models with perfect anticorrelation for $\theta = 0$, because we are interested in distinguishing LHV models from the quantum singlet state, which produces perfect anticorrelations for $\theta = 0$. Of course, there is a symmetry in the space of LHV models given by exchanging the colors of one qubit's sphere, which maps $\gamma \to 1 - \gamma$ and $C_x(\theta) \to -C_x(\theta)$. The WHCMH thus also implies that $C_x(\theta) \leqslant -C_1(\theta)$ for all colorings $x \in \mathcal{X}$ with $\gamma = 1$.

It is also interesting to investigate stronger versions of the WHCMH and related questions. For instance, is it the case that for every angle $\theta \in (\theta^{\mathrm{w}}_{\max}, \frac{\pi}{2})$ there exists a coloring $x' \in \mathcal{X}$ with $\gamma = 0$ such that $C_{x'}(\theta) < C_1(\theta)$? Further, does this hypothesis still hold true (not necessarily for the same $\theta^{\mathrm{w}}_{\max}$) if we consider general local hidden variable models corresponding to independently chosen colorings for the two qubits, not constrained by any choice of the correlation parameter γ? The following theorem and lemmas, whose proofs are presented in Appendix A, give some relevant bounds.

Theorem 1. For any coloring $x \in \mathcal{X}$, any integer $N \geqslant 2$, and any $\theta \in [\frac{\pi}{2N}, \frac{\pi}{2(N-1)})$, we have $C_1(\frac{\pi}{2N}) \leqslant C_x(\theta) \leqslant -C_1(\frac{\pi}{2N})$.

Remark 3. In particular, for small θ, $-C_1(\theta)$ and $C_1(\theta)$ are very close to the maximal possible correlation and anticorrelation for any LHVT, respectively.

Lemma 3. If any coloring $x \in \mathcal{X}$ obeys $C_x(\theta) < C_1(\theta)$ $[C_x(\theta) > -C_1(\theta)]$ for some $\theta \in (\frac{\pi}{M+1}, \frac{\pi}{M}]$ and an integer $M \geqslant 2$ then there are angles $\theta_j \equiv \frac{\pi}{M+1-j} - \theta$ with $j = 1,2,\ldots,M-1$, which satisfy $0 \leqslant \theta_j < \theta$ if $j < \frac{M}{2} + 1$ and $\frac{\pi}{2} > \theta_j > \theta$ if $j \geqslant \frac{M}{2} + 1$, such that $C_x(\theta_j) > C_1(\theta_j)$ $[C_x(\theta_j) < -C_1(\theta_j)]$.

Remark 4. In this sense (at least), the anticorrelations defined by C_1 and the correlations defined by $-C_1$ cannot be dominated by any other colorings.

Lemma 4. For any coloring $x \in \mathcal{X}$ and any $\theta \in (0, \frac{\pi}{3})$, we have $Q(\theta) < C_x(\theta) < -Q(\theta)$.

Remark 5. This inequality separates all possible LHV correlations $C_x(\theta)$ from the singlet-state quantum correlations $Q(\theta)$ for all $\theta \in (0, \frac{\pi}{3})$.

The previous observations motivate the strong hemispherical coloring maximality hypothesis (SHCMH).

The SHCMH. There exists an angle $\theta^{\mathrm{s}}_{\mathrm{max}} \in (0, \frac{\pi}{2})$ such that for every coloring $x \in \mathcal{X}$ and every angle $\theta \in [0, \theta^{\mathrm{s}}_{\mathrm{max}}]$, $C_1(\theta) \leqslant C_x(\theta) \leqslant -C_1(\theta)$.

Note that the SHCMH applies to all colorings, without any assumption of perfect anticorrelation for $\theta = 0$. If the SHCMH is true, then so is the WHCMH. In this case, we have that $\theta^{\mathrm{s}}_{\mathrm{max}} \leqslant \theta^{\mathrm{w}}_{\mathrm{max}}$. Thus, an upper bound on $\theta^{\mathrm{w}}_{\mathrm{max}}$ implies an upper bound on $\theta^{\mathrm{s}}_{\mathrm{max}}$.

IV. NUMERICAL RESULTS

We investigated the WHCMH numerically by computing the correlation $C_x(\theta)$ for various coloring functions that satisfy the antipodal property (2) and the condition (6) and that have azimuthal symmetry (see Fig. 1). Details of our numerical work are given in Appendix C. Our numerical results are consistent with the WHCMH for $\theta^{\mathrm{w}}_{\mathrm{max}} \leqslant 0.386\pi$ and with the SHCMH for $\theta^{\mathrm{s}}_{\mathrm{max}} \leqslant 0.375\pi$, but do not give strong evidence for these values. Nor do the numerical results *per se* constitute compelling evidence for the WHCMH and SHCMH, although they confirm that the underlying intuitions hold for some simple colorings.

We note that the slightly improved bound $\theta^{\mathrm{s}}_{\mathrm{max}} \leqslant 0.345\pi$ was obtained in [18]. Further details are given in Appendix C.

V. RELATED QUESTIONS FOR EXPLORATION

An interesting related question is the following: For an arbitrary two-qubit state ρ and qubit projective measurements performed by Alice and Bob corresponding to random Bloch vectors separated by an angle θ, what are the maximum values of the quantum correlations and anticorrelations $Q_\rho(\theta)$ and which states achieve them? We show that the maximum quantum anticorrelations and correlations are $Q_\rho(\theta) = -\cos\theta$, achieved by the singlet state $\rho = |\Psi^-\rangle\langle\Psi^-|$, and $Q_\rho(\theta) = \frac{1}{3}\cos\theta$, achieved by the other Bell states $\rho = |\Phi^\pm\rangle\langle\Phi^\pm|$ and $\rho = |\Psi^+\rangle\langle\Psi^+|$, respectively. This result follows because, as we show in Appendix B, we have

$$-\cos\theta \leqslant Q_\rho(\theta) \leqslant \tfrac{1}{3}\cos\theta. \tag{7}$$

Another related question that we do not explore further here is the following: For a fixed given angle θ separating Alice's and Bob's measurement axes, what are the maximum correlations and anticorrelations if, in addition to the two-qubit state ρ, Alice and Bob have other resources? For example, Alice and Bob could have an arbitrary entangled state on which they perform arbitrary local quantum operations and measurements. In a different scenario, Alice and Bob could have some amount of classical or quantum communication. Another possibility is for Alice and Bob to share arbitrary no-signaling resources, not necessarily quantum, with no communication allowed. Different variations of the task described above with continuous parameters can be investigated.

One might ask what constraints the no-signaling principle places on the correlations and anticorrelations. A generalized Popescu-Rohrlich box [19] gives the correlation $C(\theta) = \mathrm{sgn}[\pi/2 - \theta)]$, which in one natural sense defines the strongest correlations consistent with Eq. (3). Another relevant observation is that the antipodal property (3), expressed in the equivalent form $C(\pi - \theta) = -C(\theta)$, together with a continuity assumption, implies that quantum nonlocal correlations are not dominated [20]: If a correlation $C(\theta)$ produces a violation of the CHSH inequality stronger than the violation given by the singlet-state quantum correlation $Q(\theta)$ for a given set of measurement axes then there exists another set of measurement axes for which $C(\theta)$ gives a violation (or none) that is weaker than the violation given by $Q(\theta)$. It would be interesting to clarify further the relationship between measures of nonlocality, including those investigated here, and no signaling. Other related questions are given in Appendix B.

VI. DISCUSSION

We have explored here what can be learned by carrying out local projective measurements about completely randomly chosen axes, separated by an angle θ, on a pair of qubits. This is not currently a standard way of testing for entanglement or nonlocality, but we have shown that it distinguishes quantum correlations from those predicted by local hidden variables for a wide range of θ. In particular, we find Bell inequalities for $\theta \in (0, \frac{\pi}{2})$, given by Theorem 1, which separate the singlet-state quantum correlations from all LHV correlations for $\theta \in (0, \frac{\pi}{3})$.

We have also explored hypotheses that would refine and unify these results further: the weak and strong hemispherical coloring maximality hypotheses. These state that the LHV defined by the simplest spherical coloring, with opposite hemispheres colored oppositely, maximizes the LHV anticorrelations for a continuous range of $\theta > 0$, either among LHVs with perfect anticorrelation at $\theta = 0$ (the weak case) or without any restriction (the strong case).

We should note here that the intuition supporting the WHCMH relates specifically to colorings in two or more dimensions, where there seems no obvious way of constructing colorings that vary over small scales in a way that is regular enough to produce very strong (anti)correlations for small θ. On the other hand, the one-dimensional analog of the WHCMH, that the strongest anticorrelations for colorings on the circle arise from coloring opposite half circles oppositely, is easily seen to be false. For n odd, the coloring $a(\epsilon) = -b(\epsilon) = (-1)^{\lfloor n\epsilon/\pi \rfloor}$ with $\epsilon \in [0, 2\pi]$ is antipodal and is perfectly anticorrelated for $\theta = \frac{2\pi}{n}$.

Although it underlines that the hemispherical coloring hypotheses are nontrivial, this distinction between one and higher dimensions is consistent with what is known about other coloring problems in geometric combinatorics [21,22]. The intuition that coloring 1 should be optimal, because it solves the isoperimetric problem of finding the colored region with half the area of the sphere that has the shortest boundary, remains suggestive. Verifying the WHCMH and the SHCMH look at first sight like simple classical problems in geometry

and combinatorics that can be stated quite independently of quantum theory. They have many interesting generalizations.[2] Nonetheless, as far as we are aware, these questions have not been seriously studied by pure mathematicians to date, although some intriguing relatively recent results [21,22] on colorings in $\mathbb{R}^n$ encourage hope that proof methods could indeed be found. We thus simply state the WHCMH and the SHCMH as interesting and seemingly plausible hypotheses to be investigated further rather than offering them as conjectures, preferring to reserve the latter terms for propositions for which very compelling evidence has been amassed.

We would like to stress what we see as a key insight deserving further exploration, namely, that stronger and more general Bell inequalities could in principle be proven by results about continuous colorings, rather than restricting the results to colorings of discrete sets. While we have focused on the simplest case of projective measurements of pairs of qubits, this observation of course applies far more generally. We hope our work will stimulate further investigation of the WHCMH and the SHCMH and related coloring problems, which seem very interesting in their own right, and in developing further this intriguing link between natural questions in geometric combinatorics and measures of quantum nonlocality.

We have considered here the ideal case in which Alice and Bob share a maximally entangled pure state and are able to carry out perfect projective measurements about axes specified with perfect precision. For a range of nonzero θ, our results show a finite separation between the predictions of quantum theory and LHVTs. As is the case for CHSH and other Bell tests, they can thus also be applied (within a certain parameter range) to realistic experiments in which the entangled state is mixed and measurements can only be approximately specified. In particular, they offer methods for exploring the range of parameters for which the correlations defined by rotationally symmetric Werner states can be distinguished from those of any LHVT [23–26]. It would be interesting to explore this further.

Finally, but importantly, we would like to note earlier work on related questions. In a pioneering paper, Żukowski [27] considered generalized Bell and Greenberger-Horne-Zeilinger tests for maximally entangled quantum states that involve all possible axis choices and gave an elegant proof that the quantum correlations can be distinguished from all possible LHVT correlations by a weighted average measure of correlation functions. For the bipartite case, our work investigates the gap between quantum and LHVT correlations at each axis angle separation. This allows one to define infinitely many generalized Bell tests corresponding to different weighted averages of correlation functions. It would be interesting to characterize the space of all such tests and its boundaries.

References [28–30] investigate *inter alia* Bell-CHSH experiments in which the axes are initially chosen randomly and the same axes are used repeatedly throughout a given experimental run. Reference [28] shows that such experiments lead to Bell inequality violations a significant fraction of the time when pairs of random local measurements are chosen. References [29,30] show that by considering triads of random local measurements, constrained to be mutually unbiased, for which Alice's axes are not perfectly aligned to Bob's axes, the violation of a CHSH inequality is guaranteed on a two-qubit maximally entangled state. Their scenarios are significantly different from ours. In our scenario, the axes are chosen randomly and independently for each measurement and (in the ideal case) Alice and Bob have the ability to define their axis choices precisely with respect to the same reference frame. The goals are also different: References [28–30] show that Bell inequality violation can be demonstrated even when Alice and Bob do not have a shared reference frame; our aim is to establish different Bell inequalities rather than to exploit the power of known inequalities. It would be interesting to explore possible connections, nonetheless. Recently, our attention was also drawn to a related question considered in [31]; see Appendix B for discussion.

ACKNOWLEDGMENTS

We thank Boris Bukh for very helpful discussions and for drawing our attention to Refs. [21,22]. A.K. was partially supported by a grant from the John Templeton Foundation and by Perimeter Institute for Theoretical Physics. Research at Perimeter Institute is supported by the Government of Canada through Industry Canada and by the Province of Ontario through the Ministry of Research and Innovation. D.P.-G. thanks Tony Short, Boris Groisman, and Jonathan Barrett for helpful discussions and acknowledges financial support from CONACYT México and partial support from Gobierno de Veracruz.

APPENDIX A: PROOFS OF THE THEOREM AND LEMMAS

1. Proof of Lemma 1

From the CHSH inequality

$$|C(0,0) + C(1,1) + C(1,0) - C(0,1)| \leqslant 2, \tag{A1}$$

in the case in which the measurements $A = 0$, $A = 1$, and $B = 0$ correspond to projections on states with Bloch vectors separated from each other by the same angle $\theta \in (0, \frac{2\pi}{3}]$, Bob's measurement $B = 1$ is the same as Alice's measurement $A = 0$, and the outcomes are described by the LHVTs satisfying (4), we obtain after averaging over random rotations of the Bloch sphere that $|3C_x(\theta) - C_x(0)| \leqslant 2$. Then the result follows because, as shown in the main text, we have $C_x(0) = -1 + 2\gamma$.■

2. Proof of Lemma 2

From the Braunstein-Caves inequality (1) we have that

$$I_N = \left| \sum_{k=0}^{N-1} C(k,k) + \sum_{k=0}^{N-1} C(k+1,k) \right| \leqslant 2N - 2, \tag{A2}$$

[2]For example, among nonantipodal bipartite colorings of the sphere in which the black region has area $A < 2\pi$, which coloring or colorings produce maximal correlation? Alternatively, consider a general region R of volume V in $\mathbb{R}^n$ and define $p_\epsilon(R)$ to be the probability that, given a randomly chosen point $x \in R$ and a randomly chosen point y such that $d(x,y) = \epsilon$, we find that $y \in R$. Do the balls maximize this probability, for any given sufficiently small ϵ?

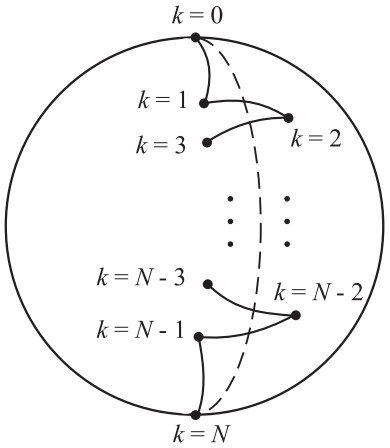

FIG. 2. Diagram of the measurements performed by Alice and Bob that are used in the proof of Lemma 2. Alice's and Bob's measurements k are the same for $k = 0,1,\ldots,N-1$ and $N \geqslant 2$; these are projections onto the states $|\xi_k\rangle$ and correspond to points in the Bloch sphere with label k. These points form a zigzag path crossing the dashed great circle. The state $|\xi_N\rangle$ is antipodal to $|\xi_0\rangle$ and represents the measurement $k = 0$ with reversed outcomes. The solid lines represent arcs of great circles with the same angle $\theta > \frac{\pi}{N}$ that connect adjacent points. If $\theta = \frac{\pi}{N}$, all these points are on the same great circle.

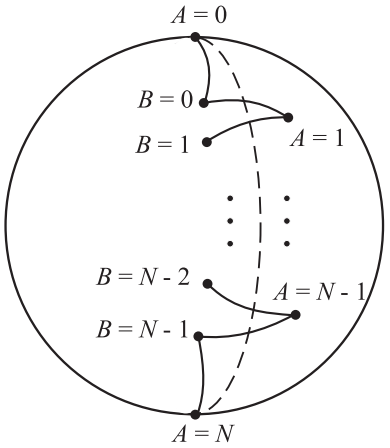

FIG. 3. Diagram of the measurements performed by Alice and Bob that are used in the proof of Theorem 1. Alice's and Bob's measurements A and B are projections onto the state $|\xi_A\rangle$ and $|\chi_B\rangle$ and correspond to points in the Bloch sphere with labels A and B, respectively, for $A,B \in \{0,1,\ldots,N-1\}$ and $N \geqslant 2$. These points form a zigzag path crossing the dashed great circle. The state $|\xi_N\rangle$ is antipodal to $|\xi_0\rangle$ and represents Alice's measurement $A = 0$ with reversed outcomes. The solid lines represent arcs of great circles with the same angle $\theta > \frac{\pi}{2N}$ that connect adjacent points. If $\theta = \frac{\pi}{2N}$, all these points are on the same great circle.

with the convention that measurement choice N is measurement choice 0 with reversed outcomes. We consider the case in which Alice's and Bob's measurements k are the same, for $k = 0,1,\ldots,N-1$ and $N \geqslant 2$, and their outcomes are described by the LHVTs satisfying (4) and (5), which then also satisfy $C_x(0) = -1 + 2\gamma$. If we take the measurement k to be of the projection onto the state $|\xi_k\rangle$ so that the states $\{|\xi_k\rangle\}_{k=0}^{N-1}$ are along a great circle on the Bloch sphere with a separation angle $\theta = \frac{\pi}{N}$ between $|\xi_k\rangle$ and $|\xi_{k+1}\rangle$ for $k = 0,1,\ldots,N-2$, for example, $|\xi_k\rangle = \cos(\frac{k\pi}{2N})|0\rangle + \sin(\frac{k\pi}{2N})|1\rangle$, and average over random rotations of the Bloch sphere, this gives

$$|NC_x(0) + NC_x(\theta)| \leqslant 2N - 2. \tag{A3}$$

Since $C_x(0) = -1 + 2\gamma$, it follows that $C_x(\frac{\pi}{N}) \geqslant -1 + \frac{2}{N} - 2\gamma = C_1(\frac{\pi}{N}) - 2\gamma$. Similarly, if we take the states $\{|\xi_k\rangle\}_{k=0}^{N-1}$ to be along a zigzag path crossing a great circle on the Bloch sphere with a separation angle $\theta > \frac{\pi}{N}$ between $|\xi_k\rangle$ and $|\xi_{k+1}\rangle$ for $k = 0,1,\ldots,N-2$ in such a way that the angle separation between $|\xi_{N-1}\rangle$ and the state with Bloch vector antiparallel to that of $|\xi_0\rangle$ is also θ (see Fig. 2), we obtain after averaging over random rotations of the Bloch sphere that $C_x(\theta) \geqslant -1 + \frac{2}{N} - 2\gamma = C_1(\frac{\pi}{N}) - 2\gamma$. ■

3. Proof of Theorem 1

Consider the Braunstein-Caves inequality (1) in the case in which Alice's and Bob's measurement outcomes are described by the LHVTs satisfying (4). Let Alice's and Bob's measurements k correspond to the projections onto the states $|\xi_k\rangle$ and $|\chi_k\rangle$, respectively, for $k = 0,1,\ldots,N-1$ and $N \geqslant 2$. Let the angle along the great circle in the Bloch sphere passing through the states $|\xi_k\rangle$ and $|\chi_k\rangle$ be θ for $k = 0,1,\ldots,N-1$. Similarly, let the angle along the great circle passing through $|\chi_k\rangle$ and $|\xi_{k+1}\rangle$ be θ for $k = 0,1,\ldots,N-1$, with the convention that the state $|\xi_N\rangle$ has a Bloch vector antiparallel to that of $|\xi_0\rangle$. If $\theta = \frac{\pi}{2N}$, all these states are on the same great circle beginning at $|\xi_0\rangle$ and ending at $|\xi_N\rangle$. If $\theta > \frac{\pi}{2N}$, the states can be accommodated on a zigzag path crossing the great circle that goes from $|\xi_0\rangle$ to $|\xi_N\rangle$ (see Fig. 3). Thus, from the Braunstein-Caves inequality, after averaging over random rotations of the Bloch sphere, we have $C_1(\frac{\pi}{2N}) = -1 + \frac{1}{N} \leqslant C_x(\theta) \leqslant 1 - \frac{1}{N} = -C_1(\frac{\pi}{2N})$ for $\theta \geqslant \frac{\pi}{2N}$. ■

4. Proof of Lemma 3

Consider a coloring $x \in \mathcal{X}$ and an angle $\theta \in (\frac{\pi}{M+1}, \frac{\pi}{M}]$ for an integer $M \geqslant 2$ such that $C_x(\theta) < C_1(\theta)$ or $C_x(\theta) > -C_1(\theta)$. From Theorem 1 and the fact that $C_x(\frac{\pi}{2}) = C_1(\frac{\pi}{2}) = 0$, it must be that $\theta \neq \frac{\pi}{M}$ if M is even. We define the angles $\theta_j \equiv \frac{\pi}{M+1-j} - \theta$ with $j = 1,2,\ldots,M-1$. Considering the cases M even and M odd and using that $\theta \neq \frac{\pi}{M}$ if M is even, it is straightforward to obtain that $0 \leqslant \theta_j < \theta$ if $j < \frac{M}{2} + 1$ and $\frac{\pi}{2} > \theta_j > \theta$ if $j \geqslant \frac{M}{2} + 1$. Now consider the Braunstein-Caves inequality (1) in the case in which Alice's and Bob's measurement outcomes are described by the LHVTs satisfying (4). Let Alice's and Bob's measurements k correspond to the projections onto the states $|\xi_k\rangle$ and $|\chi_k\rangle$, respectively, for $k = 0,1,\ldots,N-1$ and $N \equiv M + 1 - j$. Since $1 \leqslant j \leqslant M-1$, we have $2 \leqslant N \leqslant M$. Let all these states be on the great circle in the Bloch sphere that passes through the states $|\xi_0\rangle$ and $|\xi_N\rangle$, with the convention that the state $|\xi_N\rangle$ has Bloch vector antiparallel to that one of $|\xi_0\rangle$. Let the angles between $|\xi_k\rangle$ and $|\chi_k\rangle$ and between $|\chi_k\rangle$ and $|\xi_{k+1}\rangle$ along this great circle be θ and θ_j, respectively. For example, $|\xi_k\rangle = \cos(\frac{k\pi}{2N})|0\rangle + \sin(\frac{k\pi}{2N})|1\rangle$ and $|\chi_k\rangle = \cos(\frac{k\pi}{2N} + \frac{\theta}{2})|0\rangle + \sin(\frac{k\pi}{2N} + \frac{\theta}{2})|1\rangle$ for

$k = 0,1,\ldots,N-1$. From the Braunstein-Caves inequality, after averaging over random rotations of the Bloch sphere, we obtain $-1+\frac{1}{N} \leqslant \frac{1}{2}[C_x(\theta)+C_x(\theta_j)] \leqslant 1-\frac{1}{N}$. Since the average angle $\bar{\theta}_j \equiv \frac{1}{2}(\theta+\theta_j)$ satisfies $\bar{\theta}_j = \frac{\pi}{2(M+1-j)} = \frac{\pi}{2N}$ and $C_1(\frac{\pi}{2N}) = -1+\frac{1}{N}$, we have $C_1(\bar{\theta}_j) \leqslant \frac{1}{2}[C_x(\theta)+C_x(\theta_j)] \leqslant -C_1(\bar{\theta}_j)$. Since $C_1(\theta)$ is a linear function of θ, it follows that $C_x(\theta_j) > C_1(\theta_j)$ if $C_x(\theta) < C_1(\theta)$. Similarly, $C_x(\theta_j) < -C_1(\theta_j)$ if $C_x(\theta) > -C_1(\theta)$. ■

5. Proof of Lemma 4

Let $x \in \mathcal{X}$ be any coloring and $\theta \in (0,\frac{\pi}{3})$. We first consider the case $\theta \in [\frac{\pi}{4},\frac{\pi}{3})$. From Theorem 1 we have $C_1(\frac{\pi}{4}) \leqslant C_x(\theta) \leqslant -C_1(\frac{\pi}{4})$. The quantum correlation for the singlet state is $Q(\theta) = -\cos\theta$. Since $Q(\theta)$ is a strictly increasing function of θ, we have $Q(\theta) < Q(\frac{\pi}{3}) = -\frac{1}{2} = C_1(\frac{\pi}{4})$ for $\theta < \frac{\pi}{3}$. Therefore, $Q(\theta) < C_x(\theta) < -Q(\theta)$ for $\theta \in [\frac{\pi}{4},\frac{\pi}{3})$. Similarly, it is easy to see that $Q(\theta) < C_x(\theta) < -Q(\theta)$ for $\theta \in [\frac{\pi}{6},\frac{\pi}{4})$. Now we consider the case $\theta \in (0,\frac{\pi}{6})$. We define $N = \lceil \frac{\pi}{2\theta} \rceil$. It follows that $\theta \in [\frac{\pi}{2N},\frac{\pi}{2(N-1)})$ for an integer $N \geqslant 4$. From Theorem 1 we have $-1+\frac{1}{N} = C_1(\frac{\pi}{2N}) \leqslant C_x(\theta) \leqslant -C_1(\frac{\pi}{2N}) = 1-\frac{1}{N}$. From the Taylor series $Q(\theta) = -1+\frac{\theta^2}{2}-\frac{\theta^4}{4!}+\frac{\theta^6}{6!}-\cdots$ it is easy to see that $Q(\theta) < -1+\frac{\theta^2}{2}$ for $0 < \theta < \sqrt{30}$. Thus, we have $Q(\frac{\pi}{2(N-1)}) < -1+\frac{1}{2}(\frac{\pi}{2(N-1)})^2$. Since $N^2 > (\frac{\pi^2}{8}+2)N-1$, it follows that $(N-1)^2 > \frac{\pi^2}{8}N$, which implies that $-1+\frac{1}{N} > -1+\frac{1}{2}(\frac{\pi}{2(N-1)})^2$. It follows that $C_x(\theta) > Q(\frac{\pi}{2(N-1)})$. Since $Q(\theta)$ is a strictly increasing function of θ and $\theta < \frac{\pi}{2(N-1)}$, we have $Q(\frac{\pi}{2(N-1)}) > Q(\theta)$. Thus, we have $C_x(\theta) > Q(\theta)$. Similarly, we have $C_x(\theta) < -Q(\theta)$. ■

APPENDIX B: RELATED QUESTIONS FOR EXPLORATION

As mentioned in the main text, some interesting related questions involving nonlocal games with continuous inputs have been considered in [31]. In particular, in the third game considered in [31], Alice and Bob are given uniformly distributed Bloch-sphere vectors $\vec{r}_A$ and $\vec{r}_B$ and aim to maximize the probability of producing outputs that are anticorrelated if $\vec{r}_A \cdot \vec{r}_B \geqslant 0$ or correlated if $\vec{r}_A \cdot \vec{r}_B < 0$. Aharon *et al.* suggest that the LHV strategy defined by opposite hemispherical colorings is optimal, though they give no argument. They also suggest that the quantum strategy given by sharing a singlet and carrying out measurements corresponding to the input vectors is optimal, based on evidence from semidefinite programming. Equation (7) shows that this is the case for all θ and in particular for the average advantage in the game considered, if Alice and Bob are restricted to outputs defined by projective measurements on a shared pair of qubits. Our earlier results also prove that there is a quantum advantage for all θ in the range $0 < \theta < \frac{\pi}{3}$ and hence for many versions of this game defined by a variety of probability distributions for the inputs.

We show the derivation of Eq. (7) below. First, we compute the average outcome probabilities when Alice and Bob apply local projective measurements on a two-qubit state ρ for measurement bases defined by Bloch vectors separated by an angle θ. The average is taken over random rotations of these vectors in the Bloch sphere, subject to the angle separation θ. Then we compute the quantum correlations.

Consider a fixed pair of pure qubit states $|0\rangle$ and $|\chi\rangle = \cos(\frac{\theta}{2})|0\rangle + \sin(\frac{\theta}{2})|1\rangle$ for Alice's and Bob's measurements, respectively, corresponding to outcome +1. A general state for Bob's measurement separated by an angle θ with respect to a fixed state $|0\rangle$ for Alice's measurement is obtained by applying the unitary $R_z(\omega)$ that corresponds to a rotation of an angle $\omega \in [0,2\pi]$ around the z axis in the Bloch sphere, which only adds a phase to the state $|0\rangle$. Then, after applying $R_z(\omega)$, a general pure product state $|\xi_{\vec{a}}\rangle \otimes |\chi_{\vec{b}}\rangle$ of two qubits with Bloch vectors separated by an angle θ is obtained by applying the unitary $R_z(\phi)R_y(\epsilon)$ that rotates the Bloch sphere around the y axis by an angle $\epsilon \in [0,\pi]$ and then around the z axis by an angle $\phi \in [0,2\pi]$. Thus, we have $|\xi_{\vec{a}}\rangle \otimes |\chi_{\vec{b}}\rangle = U_{\phi,\epsilon,\omega}|0\rangle \otimes U_{\phi,\epsilon,\omega}|\chi\rangle$, with $U_{\phi,\epsilon,\omega} = R_z(\phi)R_y(\epsilon)R_z(\omega)$. This is a general unitary acting on a qubit, up to a global phase. Therefore, we can parametrize this unitary by the Haar measure μ on SU(2), hence, we have $|\xi_{\vec{a}}\rangle \otimes |\chi_{\vec{b}}\rangle = U_\mu|0\rangle \otimes U_\mu|\chi\rangle$.

After taking the average, the probability that both Alice and Bob obtain the outcome +1 is

$$\begin{aligned} P(++|\theta) &= \int d\mu\, \mathrm{Tr}[\rho(|\xi_{\vec{a}}\rangle\langle\xi_{\vec{a}}| \otimes |\chi_{\vec{b}}\rangle\langle\chi_{\vec{b}}|)] \\ &= \int d\mu\, \mathrm{Tr}[\rho(U_\mu \otimes U_\mu)(|0\rangle\langle 0| \otimes |\chi\rangle\langle\chi|) \\ &\quad \times (U_\mu^\dagger \otimes U_\mu^\dagger)] \\ &= \mathrm{Tr}\Big(\int d\mu (U_\mu^\dagger \otimes U_\mu^\dagger)\rho(U_\mu \otimes U_\mu) \\ &\quad \times (|0\rangle\langle 0| \otimes |\chi\rangle\langle\chi|)\Big) \\ &= \mathrm{Tr}[\tilde{\rho}(|0\rangle\langle 0| \otimes |\chi\rangle\langle\chi|)], \end{aligned} \tag{B1}$$

where in the third line we used the linearity and the cyclicity of the trace and in the fourth line we used the definition $\tilde{\rho} \equiv \int d\mu (U_\mu^\dagger \otimes U_\mu^\dagger)\rho(U_\mu \otimes U_\mu)$. The state $\tilde{\rho}$ is invariant under a unitary transformation $U \otimes U$ for any $U \in \mathrm{SU}(2)$. The only states with this symmetry are the Werner states [23], which for the two-qubit case have the general form

$$\begin{aligned} \tilde{\rho} = r|\Psi^-\rangle\langle\Psi^-| + \frac{1-r}{3}(|\Psi^+\rangle\langle\Psi^+| + |\Phi^+\rangle\langle\Phi^+| \\ + |\Phi^-\rangle\langle\Phi^-|), \end{aligned} \tag{B2}$$

with $0 \leqslant r \leqslant 1$. Thus, from Eqs. (B1) and (B2) we obtain

$$P(++|\theta) = \frac{1-r}{3} + \frac{4r-1}{6}\sin^2\left(\frac{\theta}{2}\right). \tag{B3}$$

Since the projectors corresponding to Alice and Bob obtaining outcomes -1 are obtained by a unitary transformation of the form $U \otimes U$ on $|0\rangle \otimes |\chi\rangle$, with $U \in \mathrm{SU}(2)$, then from Eq. (B1) we see that after integrating over the Haar measure on SU(2), we obtain $P(--|\theta) = P(++|\theta)$. Thus, the average quantum correlation is $Q_\rho(\theta) = 4P(++|\theta) - 1$, which from Eq. (B3) gives

$$Q_\rho(\theta) = -\left(\frac{4r-1}{3}\right)\cos\theta. \tag{B4}$$

Then Eq. (7) follows because $0 \leqslant r \leqslant 1$.

APPENDIX C: NUMERICAL RESULTS

We investigated the WHCMH numerically by computing the correlation $C_x(\theta)$ for various coloring functions that satisfy the antipodal property (2) and the condition (6) and have azimuthal symmetry. These colorings are illustrated in Fig. 1 and are defined in Appendix C 1.

We define (ϵ,ϕ) as the spherical coordinates of $\vec{a}$ and (α,β) as those of $\vec{b}$, where $\epsilon,\alpha \in [0,\pi]$ are angles from the north pole and $\phi,\beta \in [0,2\pi]$ are azimuthal angles. The vectors $\vec{a}$ and $\vec{b}$ are separated by a fixed angle θ. The set of possible values of $\vec{b}$ around the fixed axis $\vec{a}$ generate a circle parametrized by an angle ω (see Fig. 4). The spherical coordinates (α,β) for a point $\vec{b}$ with angular coordinate ω on this circle are

$$\alpha = \arccos(\cos\theta\cos\epsilon - \sin\theta\sin\epsilon\cos\omega), \tag{C1}$$

$$\beta = \left[\phi + k_\omega \arccos\left(\frac{\cos\epsilon\sin\theta\cos\omega + \sin\epsilon\cos\theta}{\sin\alpha}\right)\right] \times \mod 2\pi, \tag{C2}$$

where $k_\omega = 1$ if $0 \leqslant \omega \leqslant \pi$ and $k_\omega = -1$ if $\pi < \omega \leqslant 2\pi$. Notice that β is undefined for $\alpha \in \{0,\pi\}$.

Equations (C1) and (C2) were used to compute the double integral in (4). The integral with respect to the angle ω was performed analytically. Thus, the correlations $C_x(\theta)$ were reduced to a sum of terms that include single integrals with respect to the polar angle ϵ; the obtained expressions are given in Appendix C 2. The single integrals with respect to ϵ were computed numerically with a program using the software *Mathematica*, which we provide in Ref. [32].

Our results are plotted in Fig. 5; they are consistent with the WHCMH. They also show that $\theta^{\mathrm{w}}_{\max} < \frac{\pi}{2}$, because they show that there exists a coloring x with $C_x(\theta) < C_1(\theta)$ for some angles $\theta \in (0,\frac{\pi}{2})$, namely, coloring 3 for angles $\theta \in [0.405\pi,\frac{\pi}{2})$.

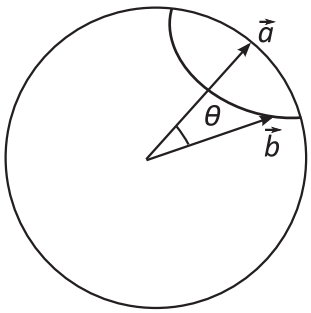

FIG. 4. Alice's and Bob's measurement axes $\vec{a}$ and $\vec{b}$ form an angle θ. The spherical coordinates of $\vec{a}$ and $\vec{b}$ are (ϵ,ϕ) and (α,β), respectively, related by Eqs. (C1) and (C2). Equation (4) computes the correlation $C_x(\theta)$ by (i) integrating the coloring function $b_x(\vec{b})$ over the circle on the sphere generated by $\vec{b}$ [parametrized by the angle ω in Eqs. (C1) and (C2)] and (ii) integrating the coloring function $a_x(\vec{a})$ over the sphere generated by $\vec{a}$. A general correlation $C(\theta) = \int_{\mathcal{X}} dx\, \mu(x) C_x(\theta)$ is computed by integrating over the probability distribution $\mu(x)$ of the colorings satisfying the antipodal property (2).

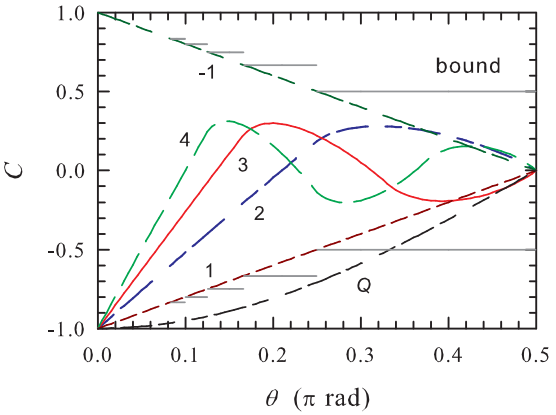

FIG. 5. (Color online) Correlations computed with (4), subject to the constraint (6), for the coloring functions a_x shown schematically in Fig. 1 and defined in Appendix C 1. The correlations for coloring 2, 3, and 4 are blue long-dash–short-dashed, red solid, and green long-dashed curves, respectively. The black long-dash–short-dashed curve represents the singlet-state quantum correlation $Q(\theta)$. The dark red short-dashed and dark green long-dash–short-dashed curves show the coloring 1 correlation $C_1(\theta)$ and anticorrelation $-C_1(\theta)$, respectively. The gray solid straight lines show the bounds given by Theorem 1 for $\theta \geqslant \frac{\pi}{12}$.

Another interesting result is that there exist colorings that produce correlations $C_x(\theta) < Q(\theta)$ for θ close to $\frac{\pi}{2}$: coloring 3 for angles $\theta \in [0.467\pi,\frac{\pi}{2})$. It is interesting to find other colorings whose correlations satisfy $C_x(\theta) < C_1(\theta)$ and $C_x(\theta) < Q(\theta)$ for angles θ closer to zero. For this purpose, we consider coloring 3_δ, which is defined in Appendix C 1 and consists of a small variation of coloring 3 in terms of the parameter δ. Coloring 3_δ reduces to coloring 3 if $\delta = 0$. For values of δ in the range $[-\frac{\pi}{18},\frac{\pi}{24}]$, we obtained that the smallest angle θ for which $C_{3_\delta}(\theta) < C_1(\theta)$ is achieved for $\delta = -0.038\pi$, in which case we have that $C_{3_{-0.038\pi}}(\theta) < C_1(\theta)$ for $\theta \in [0.386\pi,\frac{\pi}{2})$. We also obtained that the smallest angle θ for which $C_{3_\delta}(\theta) < Q(\theta)$ is achieved for $\delta = -0.046\pi$, in which case we have that $C_{3_{-0.046\pi}}(\theta) < Q(\theta)$ for $\theta \in [0.431\pi,\frac{\pi}{2})$ (see Fig. 6).

Our numerical results imply the bound $\theta^{\mathrm{w}}_{\max} \leqslant 0.386\pi$. They also imply that $\theta^{\mathrm{s}}_{\max} \leqslant 0.375\pi$, because $C_2(\theta) > -C_1(\theta)$ for $\theta \in (0.375\pi,\frac{\pi}{2})$ and $C_1(\theta) \leqslant C_x(\theta) \leqslant -C_1(\theta)$ for $x = 2,3,4,3_\delta$ and $\theta \in [0,0.375\pi]$. The slightly improved bound $\theta^{\mathrm{s}}_{\max} \leqslant 0.345\pi$ was obtained in [18] from a variation of coloring 2, coloring 2_Δ, in which the polar angle defining the boundary between the black and white regions in the northern hemisphere (see Fig. 1) is reduced by the angle $\Delta \in [0,\frac{\pi}{12}]$.

In order to confirm analytically the numerical observation that there exist coloring functions $x \in \mathcal{X}$ such that $C_x(\theta) < Q(\theta)$ for θ close to $\frac{\pi}{2}$, we computed $C_3(\frac{\pi}{2} - \tau)$ for $0 \leqslant \tau \ll 1$ to $O(\tau^2)$. The computation is presented in Appendix C 3. We obtain

$$C_3\left(\frac{\pi}{2} - \tau\right) = -1.5\tau + O(\tau^2). \tag{C3}$$

On the other hand, the quantum correlation gives $Q(\frac{\pi}{2} - \tau) = -\cos(\frac{\pi}{2} - \tau) = -\tau + O(\tau^3)$. Thus, we see that for τ small enough, indeed $C_3(\frac{\pi}{2} - \tau) < Q(\frac{\pi}{2} - \tau)$.

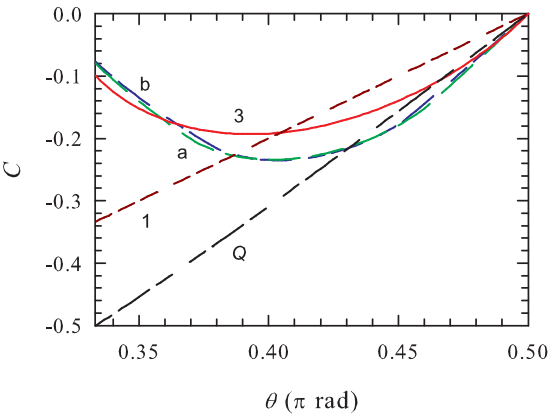

FIG. 6. (Color online) Correlations obtained for coloring 3_δ, defined in Appendix C 1, for $\delta = -0.038\pi$ (a, green dashed curve) and $\delta = -0.046\pi$ (b, blue long-dash–short-dashed curve) and for colorings 3, 1, and the singlet-state quantum correlation $Q(\theta)$ (red solid, dark red short-dashed, and black long-dash–short-dashed curves, respectively).

Further numerical investigations of the WHCMH and SHCMH might shed further light on the questions we explore here. For example, one could define an antipodal coloring function x as the sign of a sum of spherical harmonics $\mathrm{sgn}[\sum_{m=-l}^{l}\sum_{l=0}^{L} a_{lm}Y_{lm}(\epsilon,\phi)]$, where the coefficients a_{lm} are variable parameters, and then search for the minimum value of $C_x(\theta)$, for any given θ, among such functions by optimizing with respect to the a_{lm}. As an ansatz, one might assume that components corresponding to spherical harmonics that oscillate rapidly compared to θ are relatively negligible, given that the colorings defined by such functions contain black and white areas small compared to θ everywhere on the sphere, giving a contribution to the correlation very close to zero. This would allow searches over a finite set of parameters, for any given θ, while the ansatz itself can be tested by finding how the maximum changes with increasing L.

1. Definitions of the coloring functions

In general, a coloring function a_x with azimuthal symmetry can be defined in terms of the set $\mathcal{E}_x$ in which it takes the value 1 as follows:

$$a_x(\epsilon) \equiv \begin{cases} 1 & \text{if } \epsilon \in \mathcal{E}_x \\ -1 & \text{if } \epsilon \in [0,\pi]/\mathcal{E}_x, \end{cases} \tag{C4}$$

where $\epsilon \in [0,\pi]$ is the polar angle in the sphere. For the colorings that we have considered here $x = 1,2,3,4,3_\delta$, we define

$$\mathcal{E}_1 \equiv \left[0,\frac{\pi}{2}\right], \quad \mathcal{E}_2 \equiv \left[0,\frac{\pi}{4}\right]\bigcup\left[\frac{\pi}{2},\frac{3\pi}{4}\right],$$
$$\mathcal{E}_3 \equiv \bigcup_{k=0}^{2}\left[k\frac{\pi}{3},(2k+1)\frac{\pi}{6}\right], \quad \mathcal{E}_4 \equiv \bigcup_{k=0}^{3}\left[k\frac{\pi}{4},(2k+1)\frac{\pi}{8}\right],$$
$$\mathcal{E}_{3_\delta} \equiv \left[0,\frac{\pi}{6}+\delta\right]\bigcup\left[\frac{\pi}{3},\frac{\pi}{2}\right]\bigcup\left[\frac{2\pi}{3},\frac{5\pi}{6}-\delta\right], \tag{C5}$$

where $-\frac{\pi}{18} \leqslant \delta \leqslant \frac{\pi}{24}$. Notice that coloring 3_δ reduces to coloring 3 if $\delta = 0$.

2. Expressions for the correlations

We use the azimuthal symmetry of the colorings $x = 2,3,4,3_\delta$ defined in Appendix C 1, the antipodal property (2), and the constraint (6) to reduce the correlation given by (4) to

$$C_x(\theta) = -\frac{1}{\pi}\int_0^{\pi/2} d\epsilon \sin\epsilon a_x(\epsilon)\int_0^{\pi} d\omega\, a_x[\alpha(\theta,\epsilon,\omega)], \tag{C6}$$

where $\alpha(\theta,\epsilon,\omega)$ is given by Eq. (C1). We computed the integral with respect to ω in the previous expression. We define the function

$$\chi(\theta,a,b,\alpha) \equiv \frac{2}{\pi}\int_a^b d\epsilon \sin\epsilon \arccos\left(\frac{\cos\theta\cos\epsilon - \cos\alpha}{\sin\theta\sin\epsilon}\right), \tag{C7}$$

where $a,b,\alpha \in [0,\pi]$ and $\theta \in [0,\frac{\pi}{2}]$. We obtained the following expressions for the correlations $C_x(\theta)$:

$$C_2(\theta) = \begin{cases} h_2^1(\theta) & \text{if } \theta \in [0,\pi/4] \\ h_2^2(\theta) & \text{if } \theta \in (\pi/4,\pi/2], \end{cases}$$

$$C_3(\theta) = \begin{cases} h_3^1(\theta) & \text{if } \theta \in [0,\pi/6] \\ h_3^2(\theta) & \text{if } \theta \in (\pi/6,\pi/4] \\ h_3^3(\theta) & \text{if } \theta \in (\pi/4,\pi/3] \\ h_3^4(\theta) & \text{if } \theta \in (\pi/3,\pi/2], \end{cases}$$

$$C_4(\theta) = \begin{cases} h_4^1(\theta) & \text{if } \theta \in [0,\pi/8] \\ h_4^2(\theta) & \text{if } \theta \in (\pi/8,\pi/4] \\ h_4^3(\theta) & \text{if } \theta \in (\pi/4,3\pi/8] \\ h_4^4(\theta) & \text{if } \theta \in (3\pi/8,\pi/2], \end{cases}$$

$$C_{3_\delta}(\theta) = \begin{cases} r_\delta^1(\theta) & \text{if } \delta \in \left[-\frac{\pi}{18},0\right],\ \theta \in \left[\frac{\pi}{3},\frac{\pi}{3}-\delta\right] \\ r_\delta^2(\theta) & \text{if } \delta \in \left[-\frac{\pi}{18},0\right],\ \theta \in \left(\frac{\pi}{3}-\delta,\frac{\pi}{2}+\delta\right] \\ r_\delta^3(\theta) & \text{if } \delta \in \left[-\frac{\pi}{18},0\right],\ \theta \in \left(\frac{\pi}{2}+\delta,\frac{\pi}{2}\right] \\ r_\delta^4(\theta) & \text{if } \delta \in \left(0,\frac{\pi}{24}\right],\ \theta \in \left[\frac{\pi}{3},\frac{\pi}{3}+2\delta\right] \\ r_\delta^2(\theta) & \text{if } \delta \in \left(0,\frac{\pi}{24}\right],\ \theta \in \left(\frac{\pi}{3}+2\delta,\frac{\pi}{2}-\delta\right] \\ r_\delta^5(\theta) & \text{if } \delta \in \left(0,\frac{\pi}{24}\right],\ \theta \in \left(\frac{\pi}{2}-\delta,\frac{\pi}{2}\right], \end{cases} \tag{C8}$$

where

$$h_2^1(\theta) \equiv -1 + 2\left[\cos\left(\frac{\pi}{4}\right) - \cos\left(\frac{\pi}{4}+\theta\right)\right] + \chi\left(\theta,\frac{\pi}{4}-\theta,\frac{\pi}{4},\frac{\pi}{4}\right) - \chi\left(\theta,\frac{\pi}{4},\frac{\pi}{4}+\theta,\frac{\pi}{4}\right) + \chi\left(\theta,\frac{\pi}{2}-\theta,\frac{\pi}{2},\frac{\pi}{2}\right),$$

$$h_2^2(\theta) \equiv 1 + 2\left[\cos\left(\frac{\pi}{4}\right) - \cos\left(\theta - \frac{\pi}{4}\right)\right] + \chi\left(\theta,\theta - \frac{\pi}{4},\frac{\pi}{4},\frac{\pi}{4}\right) - \chi\left(\theta,\frac{\pi}{2} - \theta,\frac{\pi}{4},\frac{\pi}{2}\right) + \chi\left(\theta,\frac{\pi}{4},\frac{\pi}{2},\frac{\pi}{2}\right)$$
$$-\chi\left(\theta,\frac{\pi}{4},\frac{\pi}{2},\frac{\pi}{4}\right) - \chi\left(\theta,\frac{3\pi}{4} - \theta,\frac{\pi}{2},\frac{3\pi}{4}\right);$$

$$h_3^1(\theta) \equiv -1 + 2\left[\cos\left(\frac{\pi}{6}\right) - \cos\left(\frac{\pi}{6} + \theta\right) + \cos\left(\frac{\pi}{3}\right) - \cos\left(\frac{\pi}{3} + \theta\right)\right] + \chi\left(\theta,\frac{\pi}{6} - \theta,\frac{\pi}{6},\frac{\pi}{6}\right) - \chi\left(\theta,\frac{\pi}{6},\frac{\pi}{6} + \theta,\frac{\pi}{6}\right)$$
$$+\chi\left(\theta,\frac{\pi}{3} - \theta,\frac{\pi}{3},\frac{\pi}{3}\right) - \chi\left(\theta,\frac{\pi}{3},\frac{\pi}{3} + \theta,\frac{\pi}{3}\right) + \chi\left(\theta,\frac{\pi}{2} - \theta,\frac{\pi}{2},\frac{\pi}{2}\right),$$

$$h_3^2(\theta) \equiv 1 + 2\left[\cos\left(\frac{\pi}{6}\right) - \cos\left(\theta - \frac{\pi}{6}\right) + \cos\left(\frac{\pi}{6} + \theta\right) - \cos\left(\frac{\pi}{3}\right)\right] + \chi\left(\theta,\theta - \frac{\pi}{6},\frac{\pi}{6},\frac{\pi}{6}\right) - \chi\left(\theta,\frac{\pi}{3} - \theta,\frac{\pi}{6},\frac{\pi}{3}\right)$$
$$+\chi\left(\theta,\frac{\pi}{6},\frac{\pi}{2} - \theta,\frac{\pi}{3}\right) - \chi\left(\theta,\frac{\pi}{6},\frac{\pi}{3},\frac{\pi}{6}\right) + \chi\left(\theta,\frac{\pi}{2} - \theta,\frac{\pi}{3},\frac{\pi}{3}\right) - \chi\left(\theta,\frac{\pi}{2} - \theta,\frac{\pi}{3},\frac{\pi}{2}\right) + \chi\left(\theta,\frac{\pi}{3},\frac{\pi}{6} + \theta,\frac{\pi}{6}\right)$$
$$+\chi\left(\theta,\frac{\pi}{3},\frac{\pi}{2},\frac{\pi}{2}\right) - \chi\left(\theta,\frac{\pi}{3},\frac{\pi}{2},\frac{\pi}{3}\right) - \chi\left(\theta,\frac{2\pi}{3} - \theta,\frac{\pi}{2},\frac{2\pi}{3}\right),$$

$$h_3^3(\theta) \equiv 1 + 2\left[\cos\left(\frac{\pi}{6}\right) - \cos\left(\theta - \frac{\pi}{6}\right) + \cos\left(\frac{\pi}{6} + \theta\right) - \cos\left(\frac{\pi}{3}\right)\right] - \chi\left(\theta,\frac{\pi}{3} - \theta,\frac{\pi}{6},\frac{\pi}{3}\right) + \chi\left(\theta,\theta - \frac{\pi}{6},\frac{\pi}{6},\frac{\pi}{6}\right)$$
$$+\chi\left(\theta,\frac{\pi}{6},\frac{\pi}{3},\frac{\pi}{3}\right) - \chi\left(\theta,\frac{\pi}{6},\frac{\pi}{3},\frac{\pi}{6}\right) - \chi\left(\theta,\frac{\pi}{2} - \theta,\frac{\pi}{3},\frac{\pi}{2}\right) + \chi\left(\theta,\frac{\pi}{3},\frac{\pi}{2},\frac{\pi}{2}\right) - \chi\left(\theta,\frac{\pi}{3},\frac{\pi}{2},\frac{\pi}{3}\right)$$
$$+\chi\left(\theta,\frac{\pi}{3},\frac{\pi}{6} + \theta,\frac{\pi}{6}\right) - \chi\left(\theta,\frac{2\pi}{3} - \theta,\frac{\pi}{2},\frac{2\pi}{3}\right),$$

$$h_3^4(\theta) \equiv -1 + 2\left[\cos\left(\theta - \frac{\pi}{3}\right) - \cos\left(\frac{\pi}{6}\right) + \cos\left(\theta - \frac{\pi}{6}\right) - \cos\left(\frac{\pi}{3}\right)\right] - \chi\left(\theta,\theta - \frac{\pi}{3},\frac{\pi}{6},\frac{\pi}{3}\right) + \chi\left(\theta,\frac{\pi}{2} - \theta,\frac{\pi}{6},\frac{\pi}{2}\right)$$
$$+\chi\left(\theta,\frac{\pi}{6},\frac{\pi}{3},\frac{\pi}{3}\right) - \chi\left(\theta,\frac{\pi}{6},\frac{\pi}{3},\frac{\pi}{2}\right) - \chi\left(\theta,\theta - \frac{\pi}{6},\frac{\pi}{3},\frac{\pi}{6}\right) + \chi\left(\theta,\frac{2\pi}{3} - \theta,\frac{\pi}{3},\frac{2\pi}{3}\right)$$
$$-\chi\left(\theta,\frac{\pi}{3},\frac{\pi}{2},\frac{2\pi}{3}\right) + \chi\left(\theta,\frac{\pi}{3},\frac{\pi}{2},\frac{\pi}{2}\right) - \chi\left(\theta,\frac{\pi}{3},\frac{\pi}{2},\frac{\pi}{3}\right) + \chi\left(\theta,\frac{\pi}{3},\frac{\pi}{2},\frac{\pi}{6}\right) + \chi\left(\theta,\frac{5\pi}{6} - \theta,\frac{\pi}{2},\frac{5\pi}{6}\right);$$

$$h_4^1(\theta) \equiv -1 + 2\left[\cos\left(\frac{\pi}{8}\right) - \cos\left(\frac{\pi}{8} + \theta\right) + \cos\left(\frac{\pi}{4}\right) - \cos\left(\frac{\pi}{4} + \theta\right) + \cos\left(\frac{3\pi}{8}\right) - \cos\left(\frac{3\pi}{8} + \theta\right)\right]$$
$$+\chi\left(\theta,\frac{\pi}{8} - \theta,\frac{\pi}{8},\frac{\pi}{8}\right) - \chi\left(\theta,\frac{\pi}{8},\frac{\pi}{8} + \theta,\frac{\pi}{8}\right) + \chi\left(\theta,\frac{\pi}{4} - \theta,\frac{\pi}{4},\frac{\pi}{4}\right) - \chi\left(\theta,\frac{\pi}{4},\frac{\pi}{4} + \theta,\frac{\pi}{4}\right)$$
$$+\chi\left(\theta,\frac{3\pi}{8} - \theta,\frac{3\pi}{8},\frac{3\pi}{8}\right) - \chi\left(\theta,\frac{3\pi}{8},\frac{3\pi}{8} + \theta,\frac{3\pi}{8}\right) + \chi\left(\theta,\frac{\pi}{2} - \theta,\frac{\pi}{2},\frac{\pi}{2}\right),$$

$$h_4^2(\theta) \equiv 1 + 2\left[\cos\left(\frac{\pi}{8}\right) - \cos\left(\theta - \frac{\pi}{8}\right) + \cos\left(\theta + \frac{\pi}{8}\right) - \cos\left(\frac{\pi}{4}\right) + \cos\left(\theta + \frac{\pi}{4}\right) - \cos\left(\frac{3\pi}{8}\right)\right]$$
$$+\chi\left(\theta,\theta - \frac{\pi}{8},\frac{\pi}{8},\frac{\pi}{8}\right) - \chi\left(\theta,\frac{\pi}{4} - \theta,\frac{\pi}{8},\frac{\pi}{4}\right) + \chi\left(\theta,\frac{\pi}{8},\frac{\pi}{4},\frac{\pi}{4}\right) - \chi\left(\theta,\frac{\pi}{8},\frac{\pi}{4},\frac{\pi}{8}\right) - \chi\left(\theta,\frac{3\pi}{8} - \theta,\frac{\pi}{4},\frac{3\pi}{8}\right)$$
$$+\chi\left(\theta,\frac{\pi}{4},\frac{\pi}{8} + \theta,\frac{\pi}{8}\right) + \chi\left(\theta,\frac{\pi}{4},\frac{3\pi}{8},\frac{3\pi}{8}\right) - \chi\left(\theta,\frac{\pi}{4},\frac{3\pi}{8},\frac{\pi}{4}\right) - \chi\left(\theta,\frac{\pi}{2} - \theta,\frac{3\pi}{8},\frac{\pi}{2}\right) + \chi\left(\theta,\frac{3\pi}{8},\frac{\pi}{4} + \theta,\frac{\pi}{4}\right)$$
$$+\chi\left(\theta,\frac{3\pi}{8},\frac{\pi}{2},\frac{\pi}{2}\right) - \chi\left(\theta,\frac{3\pi}{8},\frac{\pi}{2},\frac{3\pi}{8}\right) - \chi\left(\theta,\frac{5\pi}{8} - \theta,\frac{\pi}{2},\frac{5\pi}{8}\right),$$

$$h_4^3(\theta) \equiv -1 + 2\left[\cos\left(\theta - \frac{\pi}{4}\right) - \cos\left(\frac{\pi}{8}\right) + \cos\left(\theta - \frac{\pi}{8}\right) - \cos\left(\frac{\pi}{4}\right) + \cos\left(\frac{3\pi}{8}\right) - \cos\left(\theta + \frac{\pi}{8}\right)\right]$$
$$-\chi\left(\theta,\theta - \frac{\pi}{4},\frac{\pi}{8},\frac{\pi}{4}\right) + \chi\left(\theta,\frac{3\pi}{8} - \theta,\frac{\pi}{8},\frac{3\pi}{8}\right) - \chi\left(\theta,\frac{\pi}{8},\frac{\pi}{4},\frac{3\pi}{8}\right) + \chi\left(\theta,\frac{\pi}{8},\frac{\pi}{4},\frac{\pi}{4}\right) - \chi\left(\theta,\theta - \frac{\pi}{8},\frac{\pi}{4},\frac{\pi}{8}\right)$$

$$
\begin{aligned}
&+\chi\left(\theta,\frac{\pi}{2}-\theta,\frac{\pi}{4},\frac{\pi}{2}\right)-\chi\left(\theta,\frac{\pi}{4},\frac{3\pi}{8},\frac{\pi}{2}\right)+\chi\left(\theta,\frac{\pi}{4},\frac{3\pi}{8},\frac{3\pi}{8}\right)-\chi\left(\theta,\frac{\pi}{4},\frac{3\pi}{8},\frac{\pi}{4}\right)+\chi\left(\theta,\frac{\pi}{4},\frac{3\pi}{8},\frac{\pi}{8}\right)\\
&+\chi\left(\theta,\frac{5\pi}{8}-\theta,\frac{3\pi}{8},\frac{5\pi}{8}\right)-\chi\left(\theta,\frac{3\pi}{8},\frac{\pi}{2},\frac{5\pi}{8}\right)+\chi\left(\theta,\frac{3\pi}{8},\frac{\pi}{2},\frac{\pi}{2}\right)-\chi\left(\theta,\frac{3\pi}{8},\frac{\pi}{2},\frac{3\pi}{8}\right)\\
&+\chi\left(\theta,\frac{3\pi}{8},\frac{\pi}{2},\frac{\pi}{4}\right)-\chi\left(\theta,\frac{3\pi}{8},\frac{\pi}{8}+\theta,\frac{\pi}{8}\right)+\chi\left(\theta,\frac{3\pi}{4}-\theta,\frac{\pi}{2},\frac{3\pi}{4}\right),\\
h_4^4(\theta)\equiv\ &1+2\left[\cos\left(\frac{\pi}{8}\right)-\cos\left(\theta-\frac{3\pi}{8}\right)+\cos\left(\frac{\pi}{4}\right)-\cos\left(\theta-\frac{\pi}{4}\right)+\cos\left(\frac{3\pi}{8}\right)-\cos\left(\theta-\frac{\pi}{8}\right)\right]\\
&+\chi\left(\theta,\theta-\frac{3\pi}{8},\frac{\pi}{8},\frac{3\pi}{8}\right)-\chi\left(\theta,\frac{\pi}{2}-\theta,\frac{\pi}{8},\frac{\pi}{2}\right)+\chi\left(\theta,\frac{\pi}{8},\frac{\pi}{4},\frac{\pi}{2}\right)-\chi\left(\theta,\frac{\pi}{8},\frac{\pi}{4},\frac{3\pi}{8}\right)\\
&+\chi\left(\theta,\theta-\frac{\pi}{4},\frac{\pi}{4},\frac{\pi}{4}\right)-\chi\left(\theta,\frac{5\pi}{8}-\theta,\frac{\pi}{4},\frac{5\pi}{8}\right)+\chi\left(\theta,\frac{\pi}{4},\frac{3\pi}{8},\frac{5\pi}{8}\right)-\chi\left(\theta,\frac{\pi}{4},\frac{3\pi}{8},\frac{\pi}{2}\right)\\
&+\chi\left(\theta,\frac{\pi}{4},\frac{3\pi}{8},\frac{3\pi}{8}\right)-\chi\left(\theta,\frac{\pi}{4},\frac{3\pi}{8},\frac{\pi}{4}\right)+\chi\left(\theta,\theta-\frac{\pi}{8},\frac{3\pi}{8},\frac{\pi}{8}\right)-\chi\left(\theta,\frac{3\pi}{4}-\theta,\frac{3\pi}{8},\frac{3\pi}{4}\right)\\
&+\chi\left(\theta,\frac{3\pi}{8},\frac{\pi}{2},\frac{3\pi}{4}\right)-\chi\left(\theta,\frac{3\pi}{8},\frac{\pi}{2},\frac{5\pi}{8}\right)+\chi\left(\theta,\frac{3\pi}{8},\frac{\pi}{2},\frac{\pi}{2}\right)-\chi\left(\theta,\frac{3\pi}{8},\frac{\pi}{2},\frac{3\pi}{8}\right)\\
&+\chi\left(\theta,\frac{3\pi}{8},\frac{\pi}{2},\frac{\pi}{4}\right)-\chi\left(\theta,\frac{3\pi}{8},\frac{\pi}{2},\frac{\pi}{8}\right)-\chi\left(\theta,\frac{7\pi}{8}-\theta,\frac{\pi}{2},\frac{7\pi}{8}\right);\\
r_\delta^1(\theta)\equiv\ &-1+2\left[\cos\left(\theta-\frac{\pi}{3}\right)-\cos\left(\frac{\pi}{6}+\delta\right)+\cos\left(\theta-\frac{\pi}{6}-\delta\right)-\cos\left(\frac{\pi}{3}\right)+\cos\left(\theta+\frac{\pi}{6}+\delta\right)\right]\\
&-\chi\left(\theta,\theta-\frac{\pi}{3},\frac{\pi}{6}+\delta,\frac{\pi}{3}\right)+\chi\left(\theta,\frac{\pi}{6}+\delta,\frac{\pi}{3},\frac{\pi}{3}\right)-\chi\left(\theta,\frac{\pi}{2}-\theta,\frac{\pi}{3},\frac{\pi}{2}\right)-\chi\left(\theta,\theta-\frac{\pi}{6}-\delta,\frac{\pi}{3},\frac{\pi}{6}+\delta\right)\\
&+\chi\left(\theta,\frac{2\pi}{3}-\theta,\frac{\pi}{3},\frac{2\pi}{3}\right)-\chi\left(\theta,\frac{\pi}{3},\frac{\pi}{2},\frac{2\pi}{3}\right)+\chi\left(\theta,\frac{\pi}{3},\frac{\pi}{2},\frac{\pi}{2}\right)-\chi\left(\theta,\frac{\pi}{3},\frac{\pi}{2},\frac{\pi}{3}\right)+\chi\left(\theta,\frac{\pi}{3},\theta+\frac{\pi}{6}+\delta,\frac{\pi}{6}+\delta\right),\\
r_\delta^2(\theta)\equiv\ &-1+2\left[\cos\left(\theta-\frac{\pi}{3}\right)-\cos\left(\frac{\pi}{6}+\delta\right)+\cos\left(\theta-\frac{\pi}{6}-\delta\right)-\cos\left(\frac{\pi}{3}\right)\right]-\chi\left(\theta,\theta-\frac{\pi}{3},\frac{\pi}{6}+\delta,\frac{\pi}{3}\right)\\
&+\chi\left(\theta,\frac{\pi}{2}-\theta,\frac{\pi}{6}+\delta,\frac{\pi}{2}\right)-\chi\left(\theta,\frac{\pi}{6}+\delta,\frac{\pi}{3},\frac{\pi}{2}\right)+\chi\left(\theta,\frac{\pi}{6}+\delta,\frac{\pi}{3},\frac{\pi}{3}\right)-\chi\left(\theta,\theta-\frac{\pi}{6}-\delta,\frac{\pi}{3},\frac{\pi}{6}+\delta\right)\\
&+\chi\left(\theta,\frac{2\pi}{3}-\theta,\frac{\pi}{3},\frac{2\pi}{3}\right)-\chi\left(\theta,\frac{\pi}{3},\frac{\pi}{2},\frac{2\pi}{3}\right)+\chi\left(\theta,\frac{\pi}{3},\frac{\pi}{2},\frac{\pi}{2}\right)-\chi\left(\theta,\frac{\pi}{3},\frac{\pi}{2},\frac{\pi}{3}\right)+\chi\left(\theta,\frac{\pi}{3},\frac{\pi}{2},\frac{\pi}{6}+\delta\right)\\
&+\chi\left(\theta,\frac{5\pi}{6}-\delta-\theta,\frac{\pi}{2},\frac{5\pi}{6}-\delta\right),\\
r_\delta^3(\theta)\equiv\ &-1+2\left[\cos\left(\frac{\pi}{6}+\delta\right)-\cos\left(\theta-\frac{\pi}{3}\right)+\cos\left(\frac{\pi}{3}\right)-\cos\left(\theta-\frac{\pi}{6}-\delta\right)\right]+\chi\left(\theta,\frac{\pi}{2}-\theta,\frac{\pi}{6}+\delta,\frac{\pi}{2}\right)\\
&-\chi\left(\theta,\frac{\pi}{6}+\delta,\frac{\pi}{3},\frac{\pi}{2}\right)+\chi\left(\theta,\theta-\frac{\pi}{3},\frac{\pi}{3},\frac{\pi}{3}\right)+\chi\left(\theta,\frac{2\pi}{3}-\theta,\frac{\pi}{3},\frac{2\pi}{3}\right)-\chi\left(\theta,\frac{\pi}{3},\frac{\pi}{2},\frac{2\pi}{3}\right)\\
&+\chi\left(\theta,\frac{\pi}{3},\frac{\pi}{2},\frac{\pi}{2}\right)-\chi\left(\theta,\frac{\pi}{3},\frac{\pi}{2},\frac{\pi}{3}\right)+\chi\left(\theta,\theta-\frac{\pi}{6}-\delta,\frac{\pi}{2},\frac{\pi}{6}+\delta\right)+\chi\left(\theta,\frac{5\pi}{6}-\delta-\theta,\frac{\pi}{2},\frac{5\pi}{6}-\delta\right),\\
r_\delta^4(\theta)\equiv\ &-1+2\left[\cos\left(\theta-\frac{\pi}{3}\right)-\cos\left(\theta-\frac{\pi}{6}-\delta\right)+\cos\left(\frac{\pi}{6}+\delta\right)-\cos\left(\frac{\pi}{3}\right)\right]-\chi\left(\theta,\theta-\frac{\pi}{3},\frac{\pi}{6}+\delta,\frac{\pi}{3}\right)\\
&+\chi\left(\theta,\theta-\frac{\pi}{6}-\delta,\frac{\pi}{6}+\delta,\frac{\pi}{6}+\delta\right)+\chi\left(\theta,\frac{\pi}{2}-\theta,\frac{\pi}{6}+\delta,\frac{\pi}{2}\right)-\chi\left(\theta,\frac{\pi}{6}+\delta,\frac{\pi}{3},\frac{\pi}{2}\right)+\chi\left(\theta,\frac{\pi}{6}+\delta,\frac{\pi}{3},\frac{\pi}{3}\right)\\
&-\chi\left(\theta,\frac{\pi}{6}+\delta,\frac{\pi}{3},\frac{\pi}{6}+\delta\right)+\chi\left(\theta,\frac{2\pi}{3}-\theta,\frac{\pi}{3},\frac{2\pi}{3}\right)-\chi\left(\theta,\frac{\pi}{3},\frac{\pi}{2},\frac{2\pi}{3}\right)\\
&+\chi\left(\theta,\frac{\pi}{3},\frac{\pi}{2},\frac{\pi}{2}\right)-\chi\left(\theta,\frac{\pi}{3},\frac{\pi}{2},\frac{\pi}{3}\right)+\chi\left(\theta,\frac{\pi}{3},\frac{\pi}{2},\frac{\pi}{6}+\delta\right)+\chi\left(\theta,\frac{5\pi}{6}-\delta-\theta,\frac{\pi}{2},\frac{5\pi}{6}-\delta\right),
\end{aligned}
$$

$$r_\delta^5(\theta) \equiv -1 + 2\left[\cos\left(\theta - \frac{\pi}{3}\right) - \cos\left(\frac{\pi}{6} + \delta\right) + \cos\left(\theta - \frac{\pi}{6} - \delta\right) - \cos\left(\frac{\pi}{3}\right)\right] + \chi\left(\theta, \frac{\pi}{2} - \theta, \frac{\pi}{6} + \delta, \frac{\pi}{2}\right)$$
$$- \chi\left(\theta, \theta - \frac{\pi}{3}, \frac{\pi}{6} + \delta, \frac{\pi}{3}\right) - \chi\left(\theta, \frac{2\pi}{3} - \theta, \frac{\pi}{6} + \delta, \frac{2\pi}{3}\right) + \chi\left(\theta, \frac{\pi}{6} + \delta, \frac{\pi}{3}, \frac{2\pi}{3}\right) - \chi\left(\theta, \frac{\pi}{6} + \delta, \frac{\pi}{3}, \frac{\pi}{2}\right)$$
$$+ \chi\left(\theta, \frac{\pi}{6} + \delta, \frac{\pi}{3}, \frac{\pi}{3}\right) - \chi\left(\theta, \theta - \frac{\pi}{6} - \delta, \frac{\pi}{3}, \frac{\pi}{6} + \delta\right) - \chi\left(\theta, \frac{5\pi}{6} - \delta - \theta, \frac{\pi}{3}, \frac{5\pi}{6} - \delta\right) + \chi\left(\theta, \frac{\pi}{3}, \frac{\pi}{2}, \frac{5\pi}{6} - \delta\right)$$
$$- \chi\left(\theta, \frac{\pi}{3}, \frac{\pi}{2}, \frac{2\pi}{3}\right) + \chi\left(\theta, \frac{\pi}{3}, \frac{\pi}{2}, \frac{\pi}{2}\right) - \chi\left(\theta, \frac{\pi}{3}, \frac{\pi}{2}, \frac{\pi}{3}\right) + \chi\left(\theta, \frac{\pi}{3}, \frac{\pi}{2}, \frac{\pi}{6} + \delta\right).$$

3. Proof of Eq. (C3)

Let $0 \leqslant \tau \ll 1$. To show Eq. (C3), we expand $C_3(\frac{\pi}{2} - \tau)$ in its Taylor series to obtain

$$C_3\left(\frac{\pi}{2} - \tau\right) = C_3\left(\frac{\pi}{2}\right) + \tau\left[\frac{d}{d\tau} C_3\left(\frac{\pi}{2} - \tau\right)\right]_{\tau=0} + O(\tau^2). \tag{C9}$$

As shown in the main text, the correlation satisfies $C_x(\frac{\pi}{2}) = 0$ for any pair of colorings labeled by x that we consider. Thus, we have that $C_3(\frac{\pi}{2}) = 0$. From Eq. (C8) we have that $C_3(\frac{\pi}{2} - \tau) = h_3^4(\frac{\pi}{2} - \tau)$ for $0 \leqslant \tau \ll 1$. Thus, we only need to show that

$$\left[\frac{d}{d\theta} h_3^4(\theta)\right]_{\theta=\pi/2} = 1.5. \tag{C10}$$

The function $h_3^4(\theta)$ has terms of the form

$$\chi(\theta, a, b, \alpha) \equiv \int_a^b d\epsilon\, \xi(\theta, \epsilon, \alpha), \tag{C11}$$

where

$$\xi(\theta, \epsilon, \alpha) \equiv \frac{2}{\pi} \sin\epsilon \arccos\left(\frac{\cos\theta\cos\epsilon - \cos\alpha}{\sin\theta\sin\epsilon}\right), \tag{C12}$$

as defined by Eq. (C7). Differentiating the function χ, we obtain

$$\frac{d}{d\theta}\chi(\theta, a, b, \alpha) = \xi(\theta, b, \alpha)\frac{db}{d\theta} - \xi(\theta, a, \alpha)\frac{da}{d\theta} + \int_a^b d\epsilon \frac{\partial}{\partial\theta}\xi(\theta, \epsilon, \alpha). \tag{C13}$$

We have that

$$\left[\frac{\partial}{\partial\theta}\xi(\theta, \epsilon, \alpha)\right]_{\theta=\pi/2} = \frac{2\cos\epsilon}{\pi\sqrt{1 - (\cos\alpha/\sin\epsilon)^2}}. \tag{C14}$$

We obtain that

$$\frac{2}{\pi}\int_a^b \frac{d\epsilon\cos\epsilon}{\sqrt{1 - (\cos\alpha/\sin\epsilon)^2}} = \mu(a, b, \alpha), \tag{C15}$$

where

$$\mu(a, b, \alpha) \equiv \frac{2}{\pi}\left(\sqrt{\sin^2 b - \cos^2\alpha} - \sqrt{\sin^2 a - \cos^2\alpha}\right) \tag{C16}$$

for $\cos^2\alpha \leqslant \sin^2 b$ and $\cos^2\alpha \leqslant \sin^2 a$. We define

$$\nu(\epsilon, \alpha) \equiv \xi\left(\frac{\pi}{2}, \epsilon, \alpha\right). \tag{C17}$$

From the definition of $h_3^4(\theta)$ given in Appendix C 2 and Eqs. (C13)–(C17), it is straightforward to obtain that

$$\left[\frac{d}{d\theta} h_3^4(\theta)\right]_{\theta=\pi/2} = -2\left[\sin\left(\frac{\pi}{6}\right) + \sin\left(\frac{\pi}{3}\right)\right] + \nu\left(0, \frac{\pi}{2}\right) + \nu\left(\frac{\pi}{6}, \frac{\pi}{3}\right)$$
$$+ \nu\left(\frac{\pi}{6}, \frac{2\pi}{3}\right) + \nu\left(\frac{\pi}{3}, \frac{\pi}{6}\right) + \nu\left(\frac{\pi}{3}, \frac{5\pi}{6}\right)$$
$$+ \mu\left(0, \frac{\pi}{6}, \frac{\pi}{2}\right) - \mu\left(\frac{\pi}{6}, \frac{\pi}{6}, \frac{\pi}{3}\right)$$
$$+ \mu\left(\frac{\pi}{6}, \frac{\pi}{3}, \frac{\pi}{3}\right) - \mu\left(\frac{\pi}{6}, \frac{\pi}{3}, \frac{\pi}{2}\right) + \mu\left(\frac{\pi}{6}, \frac{\pi}{3}, \frac{2\pi}{3}\right)$$
$$- \mu\left(\frac{\pi}{3}, \frac{\pi}{3}, \frac{\pi}{6}\right) + \mu\left(\frac{\pi}{3}, \frac{\pi}{2}, \frac{\pi}{2}\right) + \mu\left(\frac{\pi}{3}, \frac{\pi}{2}, \frac{\pi}{6}\right)$$
$$- \mu\left(\frac{\pi}{3}, \frac{\pi}{2}, \frac{2\pi}{3}\right) - \mu\left(\frac{\pi}{3}, \frac{\pi}{2}, \frac{\pi}{3}\right) + \mu\left(\frac{\pi}{3}, \frac{\pi}{2}, \frac{5\pi}{6}\right). \tag{C18}$$

We use Eqs. (C12), (C16), and (C17) and notice that $\nu(0, \frac{\pi}{2}) = 0$ in order to evaluate the previous expression. We obtain

$$\left[\frac{d}{d\theta} h_3^4(\theta)\right]_{\theta=\pi/2} = \frac{1}{\pi}[6 - 4(\sqrt{3} - \sqrt{2})] = 1.5, \tag{C19}$$

as claimed.

[1] J. Bell, Physics **1**, 195 (1964).

[2] A. Aspect, J. Dalibard, and G. Roger, Phys. Rev. Lett. **49**, 1804 (1982).

[3] G. Weihs, T. Jennewein, C. Simon, H. Weinfurter, and A. Zeilinger, Phys. Rev. Lett. **81**, 5039 (1998).

[4] W. Tittel, J. Brendel, H. Zbinden, and N. Gisin, Phys. Rev. Lett. **81**, 3563 (1998); N. Gisin and H. Zbinden, Phys. Lett. A **264**, 103 (1999).

[5] M. A. Rowe, D. Kielpinski, V. Meyer, C. A. Sackett, W. M. Itano, C. Monroe, and D. J. Wineland, Nature (London) **409**, 791 (2001).

[6] D. N. Matsukevich, P. Maunz, D. L. Moehring, S. Olmschenk, and C. Monroe, Phys. Rev. Lett. **100**, 150404 (2008).
[7] D. Salart, A. Baas, J. A. W. van Houwelingen, N. Gisin, and H. Zbinden, Phys. Rev. Lett. **100**, 220404 (2008).
[8] M. Giustina, A. Mech, S. Ramelow, B. Wittmann, J. Kofler, J. Beyer, A. Lita, B. Calkins, T. Gerrits, S. W. Nam, R. Ursin, and A. Zeilinger, Nature (London) **497**, 227 (2013).
[9] P. M. Pearle, Phys. Rev. D **2**, 1418 (1970).
[10] A. Kent, Phys. Rev. A **72**, 012107 (2005).
[11] J. F. Clauser, M. A. Horne, A. Shimony, and R. A. Holt, Phys. Rev. Lett. **23**, 880 (1969).
[12] A. Einstein, B. Podolsky, and N. Rosen, Phys. Rev. **47**, 777 (1935).
[13] D. Bohm, *Quantum Theory* (Prentice-Hall, Englewood Cliffs, 1951).
[14] B. S. Cirel'son, Lett. Math. Phys. **4**, 93 (1980).
[15] S. L. Braunstein and C. M. Caves, Ann. Phys. (N.Y.) **202**, 22 (1990).
[16] S. Wehner, Phys. Rev. A **73**, 022110 (2006).
[17] A. P. Kent, W. J. Munro, T. P. Spiller, and R. G. Beausoleil, U.S. Patent No. 7,983,422 (19 July 2011).
[18] D. Pitalúa-García, Ph.D. thesis, University of Cambridge, 2014.
[19] S. Popescu and D. Rohrlich, Found. Phys. **24**, 379 (1994).
[20] A. Kent, arXiv:1308.5009.
[21] B. Bukh, Geom. Funct. Anal. **18**, 668 (2008).
[22] F. M. de Oliveira Filho and F. Vallentin, J. Eur. Math. Soc. **12**, 1417 (2010).
[23] R. F. Werner, Phys. Rev. A **40**, 4277 (1989).
[24] A. Acín, N. Gisin, and B. Toner, Phys. Rev. A **73**, 062105 (2006).
[25] T. Vértesi, Phys. Rev. A **78**, 032112 (2008).
[26] N. Brunner, D. Cavalcanti, S. Pironio, V. Scarani, and S. Wehner, Rev. Mod. Phys. **86**, 419 (2014).
[27] M. Żukowski, Phys. Lett. A **177**, 290 (1993).
[28] Y.-C. Liang, N. Harrigan, S. D. Bartlett, and T. Rudolph, Phys. Rev. Lett. **104**, 050401 (2010).
[29] P. Shadbolt, T. Vértesi, Y.-C. Liang, C. Branciard, N. Brunner, and J. L. O'Brien, Sci. Rep. **2**, 470 (2012).
[30] J. J. Wallman and S. D. Bartlett, Phys. Rev. A **85**, 024101 (2012).
[31] N. Aharon, S. Machnes, B. Reznik, J. Silman, and L. Vaidman, Nat. Comput. **12**, 5 (2013).
[32] See Supplemental Material at http://link.aps.org/supplemental/10.1103/PhysRevA.90.062124 for the computer program.